International Journal of Geosciences, 2025, 16(10), 685-700
https://www.scirp.org/journal/ijg
ISSN Online: 2156-8367
ISSN Print: 2156-8359

Lithospheric Magnetic Anomaly in the Surrounding Area of the Dingri M6.8 Earthquake, Xizang

Bo Li[1,2], Fenglong Mao[1,2]

[1]Baoding Central Seismic Station of Hebei Province, Baoding, China
[2]Hebei Hongshan National Observatory on Thick Sediments and Seismic Hazards, Xingtai, China
Email: lb2007@qq.com

How to cite this paper: Li, B. and Mao, F.L. (2025) Lithospheric Magnetic Anomaly in the Surrounding Area of the Dingri M6.8 Earthquake, Xizang. *International Journal of Geosciences*, **16**, 685-700.
https://doi.org/10.4236/ijg.2025.1610034

Received: August 24, 2025
Accepted: October 12, 2025
Published: October 15, 2025

Abstract

The occurrence and development of earthquakes can cause abnormal changes in the lithospheric magnetic field. High-precision geomagnetic observations on both sides of the Dingri M6.8 epicenter revealed a −120 nT difference in the lithospheric magnetic field between the west and east sides, reflecting the local difference characteristics of the properties of the crustal medium around the epicenter. From 2018 to 2020, the annual variation of the magnetic field changed from −2.2 nT to +3.9 nT, which may be the precursor anomaly of the Dingri M5.9 earthquake in 2020. Calculations show that in the coseismic magnetic field variation of the M6.8 earthquake, the piezomagnetic effect is small while the electrokinetic effect is large, so the precursor anomaly of the M5.9 earthquake may be related to the electrokinetic effect produced by underground fluid migration.

Keywords

Dingri M6.8 Earthquake, Lithospheric Magnetic Field, Piezomagnetic Effect, Electrokinetic Effect

1. Introduction

According to the official measurement of the China Earthquake Networks Center, on January 7, 2025, a magnitude 6.8 earthquake (hereinafter referred to as the Dingri earthquake) occurred in Dingri County, Xizang, with the epicenter at (28.5˚N, 87.45˚E). This earthquake occurred on the Dengmocuo fault in the southern section of the Xainza-Dingye fault system, which runs in a nearly north-south direction [1]. It is a normal fault-type earthquake (**Figure 1**). Due to the north-south collision and east-west tension between the Indian Plate and the Eur-

asian Plate [2], multiple catastrophic earthquakes have occurred in southern Xizang, with a high seismic risk [3]. There was a 5.9 magnitude earthquake around the Dingri earthquake in 2020 [4], but there is not much research on the seismogenic environment and regional seismic risk of the Dingri 5.9 magnitude earthquake. This may be due to the high altitude of the region, the difficulty of data collection, and most of the research focusing on large fractures at the block boundaries [3]. The occurrence of the Dingri earthquake once again demonstrates that small and medium-sized faults or internal faults within blocks also have the potential to cause catastrophic earthquakes [5]. Compared to other surrounding faults, the Dengmocuo Fault has a higher activity rate, and its seismic hazard should be taken seriously [6]. On-site investigation shows that the earthquake rupture mainly occurred along the epicenter towards the north, and the maximum vertical displacement found on the surface has reached 3 m [1], indicating the significant shallow sliding and huge energy released by the 6.8 magnitude earthquake in Dingri. Therefore, using historical observation data to conduct research on regional earthquake background and basic models is of certain significance for understanding the seismic hazard of the region, and can provide a reference for subsequent geological, geophysical, and other observations.

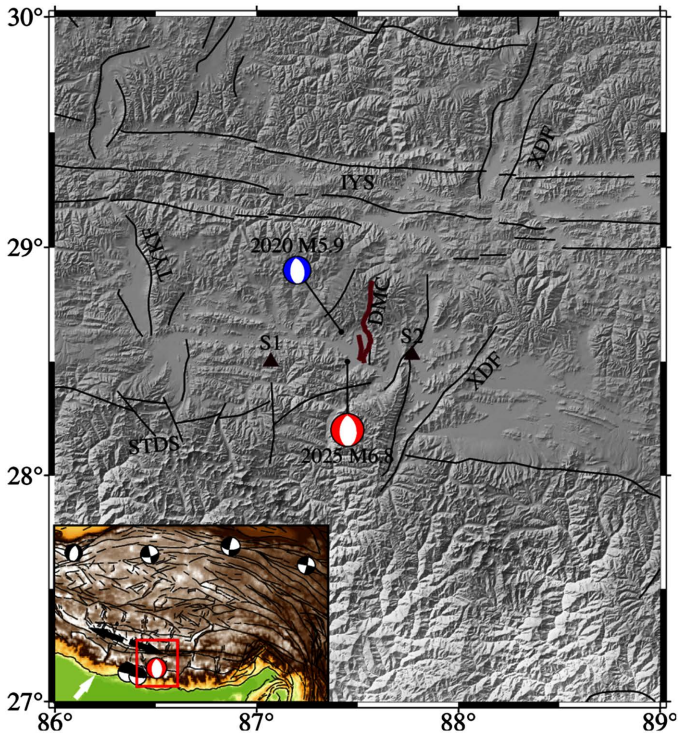

Figure 1. Tectonic setting of the research area (drawn according to the earthquake catalog of China Earthquake Networks Center).

There is a good correspondence between earthquakes and geomagnetic field anomalies. Earthquakes with a magnitude of 6.0 or above in the Sichuan-Yunnan region often occur in areas with negative anomalies at the junction of positive and

negative lithospheric magnetic fields. Recently, satellite data provides a good chance to detect pre-earthquake magnetic anomalies [7]-[10]. Many researches indicate that geomagnetic field anomalies can provide a reference for earthquake risk analysis [11]-[13]. There are few geomagnetic observation data in southern Xizang, especially in the area south of the Indus-Yarlung suture. From the fine lithospheric magnetic field model, it can only be recognized that the region is mainly a weak negative anomaly [14]. Whether the Dingri earthquake is at the boundary of positive and negative anomalies of the lithospheric magnetic field needs further research according to the measured data.

Earthquake-induced rupture or material transport related to seismogenesis can often cause disturbances in the geomagnetic field [15]-[17], providing references for earthquake prediction, earthquake warning, earthquake rupture, and other research [18] [19]. Domestic researchers have extracted multiple abnormal changes in the geomagnetic field before earthquakes through repeated observations of the geomagnetic field. These changes are usually of large magnitude, and the mechanism is not clear [20]-[22]. Unlike pre-earthquake anomaly studies, coseismic geomagnetic field anomalies exhibit characteristics of smaller magnitude and range [19]. Some persistent coseismic geomagnetic field anomalies can be quantitatively explained by the pressure magnetic effect [19] [23], which greatly inspires earthquake geomagnetic research. Some researchers believe that the abnormal geomagnetic field before earthquakes is related to the stress changes during the pre-earthquake process [22]-[24], but they have not explained the significant changes, indicating that there are huge differences between the qualitative analysis and quantitative calculation of lithospheric magnetic field anomalies, which seriously restricts the study of seismic magnetic anomalies. The large shallow sliding of the 6.8-magnitude earthquake on Dingri may cause significant coseismic geomagnetic field anomalies. Quantitative calculation of its coseismic geomagnetic changes can provide references for subsequent regional geomagnetic field analysis.

Observable seismomagnetic anomalies are correlated with both earthquake magnitude and epicentral distance. Based on analyses of case studies, Hattori *et al.* (2004) [25] proposed an empirical relationship expressed as $0.025R < M4.5$ (where R denotes epicentral distance and M represents magnitude). This implies that the maximum epicentral distances for detecting anomalies at geomagnetic stations would be approximately 60 km for M6.0 earthquakes and 100 km for M7.0 earthquakes. For earthquakes with shallow focal depths, the spatial extent of detectable geomagnetic anomalies may be larger. To study the potential anomalous characteristics of the geomagnetic field around the Dingri earthquake, this paper obtained the variation of the geomagnetic field perpendicular to the direction of the Dengmocuo fault based on repeated observation data of the geomagnetic field obtained at 30 km on both sides of the epicenter from 2018 to 2020. At the same time, based on quantitative calculations of the geomagnetic effects of synchronous earthquakes, the changes in the magnetic field of synchronous earth-

quakes were obtained, and the mechanisms of synchronous and pre-earthquake magnetic field anomalies were analyzed. No geomagnetic observations have been conducted in this region since 2020, making the latest data unavailable.

S1 and S2 are geomagnetic repeat measurement points; XDF is the Xainza-Dingye fault; TYKF is the TangraYumco-Kongco fault; DMC is the Dengmocuo fault; STDS is the Southern Tibetan Detachment System; IYS is the Indus-Yarlung suture; Beach balls in lower left subplot are earthquakes with $M_W > 7.0$ that occurred in the Qinghai-Yibet plateau; thick white arrow indicates the motion of the Indian plate relative to the Eurasian plate; black white arrows indicate the dilatation motion in the southern Qinghai-Xizang plateau; the red line area is the research area.

2. Data and Methods

From 2018 to 2020, relevant units of the China Earthquake Administration carried out a large number of repeated observations of the geomagnetic field on the Qinghai-Xizang Plateau to fill the gap in geomagnetic field observations in the region. Each measuring point is equipped with duplicate positioning markers to ensure that repeated measurements are taken at the same measuring point, with an instrument installation error of less than 10 cm. An auxiliary measuring point is set up at a distance of 20 - 30 meters from each measuring point, and the horizontal gradient of the magnetic field within 5 meters of the measuring point and the auxiliary measuring point is less than 2 nT/m, and the vertical gradient of the magnetic field within 2 meters is less than 3 nT/m. The repeat positioning error can be controlled within 0.3 nT. During each observation, double-check the magnetic field gradient at the measuring point and the magnetic field difference between the measuring point and the auxiliary measuring point to ensure that there is no obvious human interference around the measuring point. Six sets of observations of the total intensity of the geomagnetic field will be conducted within approximately 30 minutes of each measurement, with 10 values observed in each set. The observation instruments are all GSM-19T proton precession magnetometers with a sensitivity of 0.15 nT@1Hz. The resolution is 0.01 nT and the absolute accuracy is ±0.2 nT [26].

Referring to the observation data of Lhasa geomagnetic station, daily variation correction is carried out to eliminate the majority of external interference. The method is shown in formula (1). The natural orthogonal component model, based on the observation data of 36 geomagnetic stations in the Chinese Mainland, is used to correct the daily variation correction results in 2018, 2019, and 2020 to the same day, so as to eliminate the long-term variation of the geomagnetic field [27] [28]. The correction error of daily variation is related to the distance between the measuring point and the reference station [23] [29]. The distance between the Lhasa geomagnetic station and the two measuring points is about 350 km. Using the data from the Lhasa geomagnetic station for daily variation correction may result in an error of 1 - 2 nT. To eliminate this error, the difference between the

daily variation correction results of the two measurement points was calculated, which also eliminated the main magnetic field and obtained the difference dF of the lithospheric magnetic field at the two measurement points.

$$F_{obs}(t0) = F_{obs}(t) - \left(F_{ref}(t) - F_{ref}(t0)\right) \quad (1)$$

In the formula, $F_{obs}(t0)$ is the daily variation correction result of the measured value at the measuring point; $F_{obs}(t)$ is the measurement value at measuring point t at time t; $F_{ref}(t)$ is the observed value at time t at the reference station; $F_{ref}(t0)$ is the measurement value at zero point corrected for the daily variation of the reference station. The daily change correction for each period is from 00:00 to 03:00 Beijing time on a certain day.

$$dF = F_{S1} - F_{S2} \quad (2)$$

In the formula, dF represents the difference in the lithospheric magnetic field between measurement points S1 and S2, while F_{S1} and F_{S2} represent the correction results of the observed changes at observation points S1 and S2, respectively.

The main sources of data result errors are instrument installation and long-term variation correction. The data fitting accuracy of the natural orthogonal component model is better than 1 nT [17], and the instrument installation error is better than 0.3 nT. Therefore, it can be considered that the data result error is better than 1 nT.

3. Results

3.1. Lithospheric Magnetic Field and Changes

Based on the previous method, dF values from 2018 to 2020 were obtained, and the results are shown in Table 1. The difference in the lithospheric magnetic field between the two measurement points is about −120 nT, indicating the presence of significant magnetic anomalies between the two measurement points. Considering that the horizontal and vertical gradients of the two measuring points are relatively small, this anomaly cannot be a local anomaly of the measuring points, but more likely reflects the characteristics of the regional lithospheric magnetic field.

The changes in the magnetic field of the lithosphere from 2018 to 2020 were -2.2 nT in 2018-2019 and +3.9 nT in 2019-2020. The crustal compression or tension strain generated by tectonic loading in the Qinghai-Xizang Plateau region is usually around 10^{-8}, which can only produce magnetic field changes of 10^{-1} nT [30]. In the absence of severe crustal material migration, such as earthquakes and volcanic eruptions, it is generally believed that the changes in the magnetic field of the lithosphere do not change with time [28]. From 2018 to 2020, there was a change of about 6 nT in the lithospheric magnetic field, indicating that there may have been significant changes in crustal material during this period. At the same time, the reverse changes in the lithospheric magnetic field from 2018 to 2019 and from 2019 to 2020 indicate that the lithospheric magnetic field at the two measurement points experienced different effects in 2018, 2019, and 2020, thus exhibiting significant reversal changes.

Table 1. The *dF* values from 2018 to 2020.

Observed Time	2018	2019	2020
dF/nT	−118.7	−120.9	−117.0

3.2. Coseismic Piezomagnetic Effect

The seismic coseismic process is accompanied by significant stress release, which can lead to abnormal changes in the geomagnetic field, known as the piezomagnetic effect. The calculation methods for the piezomagnetic effect are divided into analytical methods and numerical calculation methods [31]. The analytical method has a small computational cost and is not prone to distortion, but it can only use uniform medium parameters. Although numerical calculation methods can consider three-dimensional medium parameters, their computational complexity is enormous and distortion may occur at fault planes. Considering the difficulty in obtaining accurate medium parameters, this section uses analytical methods to calculate the piezomagnetic field that may be generated by the Dingri earthquake. The parameters mainly include magnetization intensity (J), stress sensitivity coefficient (β), medium shear modulus (G), and sliding distribution (S) [31]. The values of β and J vary with factors such as lithology and burial depth [23], and precise determination is challenging [19]. Due to the linear relationship between the calculated piezomagnetic field and the product of magnetization and stress sensitivity coefficient (βJ) [19], both β and J can be selected as 1×10^{-9} Pa and 1 A/m to calculate the initial piezomagnetic field. When βJ changes, the final result is the initial piezomagnetic field multiplied by the corresponding multiple of βJ. The shear modulus of crustal media has an impact on the calculated piezomagnetic field [32], especially the mechanical properties of the shallow crust have a significant influence on the calculated piezomagnetic field [31]. Considering that the Dingri earthquake occurs in the crust with low wave velocity, corresponding to a P-wave velocity of about 5 km/s, the shear modulus of the crust is selected as 22 GPa. The magnetic declination and tilt angle refer to the results of IGRF14 [33], which are +0.3˚ (positive values indicate north northeast) and 45.2˚, respectively.

After the Dingri earthquake, different research institutions provided the slip distribution of coseismic faults based on seismic wave data. The rupture surface is roughly 50 to 80 km, and the rupture is mainly distributed north of the epicenter. However, the slip distribution given by different results varies greatly. Based on the preliminary results of the field survey, the surface dislocation in some areas is more than 3 m, and there is a possibility of a greater surface fault. Therefore, this paper selects a slip distribution model that is more consistent with the surface survey for calculation (from the Institute of Tibetan Plateau Research, Chinese Academy of Sciences [34], see **Figure 2**).

The calculation results of the coseismic piezomagnetic field show (see **Figure 3**) that a significant piezomagnetic field appears at the upper edge and both ends of the sliding surface, with a maximum piezomagnetic field exceeding 1 nT, re-

flecting the controlling effect of shallow stress changes on the piezomagnetic field. The majority of the area along the sliding surface has a negative piezomagnetic field, with only a small range of positive values appearing on the north side. This is because the sliding amount is mainly distributed in the area north of the sliding surface. The piezomagnetic field at the epicenter is about +0.2 nT, and the piezomagnetic fields at the two measuring points are +0.04 nT and −0.04 nT, respectively, indicating that the piezomagnetic field decays rapidly with distance. Due to the relatively small values of β and J used in this article, most studies have used β and J that are 1.5 to 3 times higher than in this article [13], that is, βJ is 3 to 10 times higher than in this article, and some studies have used larger dielectric magnetic parameters. When choosing βJ to be 3 to 10 times that of this article, the piezomagnetic field at the epicenter can reach 0.5 to 2 nT, but the piezomagnetic field at the two measuring points is still relatively small, possibly 0.1 to 0.3 nT, which is difficult to observe by instruments.

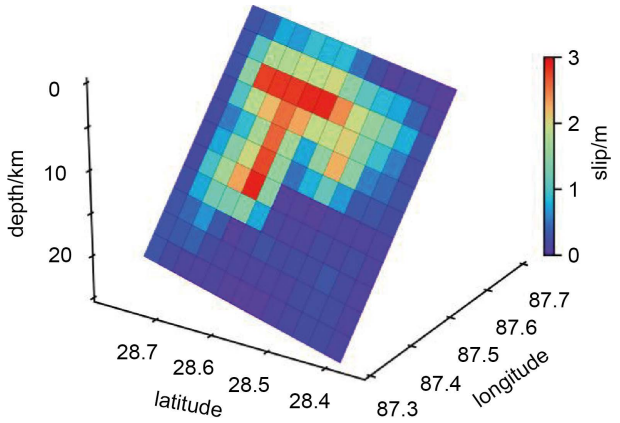

Figure 2. Coseismic slip model of Dingri M6.8 earthquake.

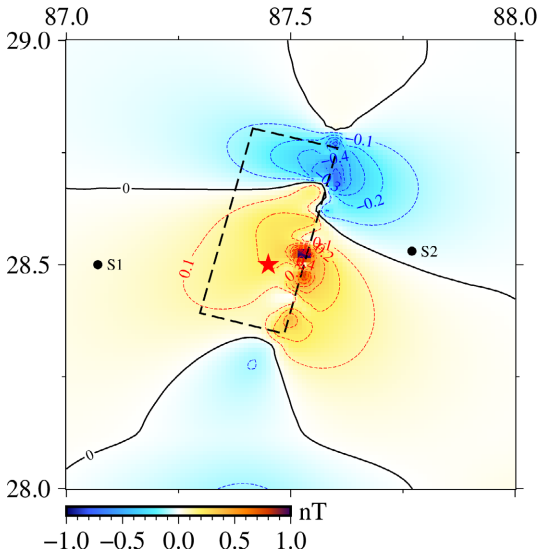

Figure 3. Coseismic piezomagnetic fields expected from Dingri M6.8 earthquake.

3.3. Coseismic Electrokinetic Effect

Another magnetic field effect related to earthquakes is the electrokinetic effect, which can generate a flowing electric potential when liquid flows through a discontinuous underground interface, thereby producing a magnetic field [35] [36]. This article is based on the analytical method of the electrokinetic effect generated by dislocation sources given in reference [36] to calculate the changes in the coseismic magnetic field of the Dingri earthquake. The model parameters include the length of the fracture surface (l), the burial depth at the top of the fracture surface (a), the burial depth at the bottom of the fracture surface (b), the conductivity on both sides of the fracture surface (σ_1 and σ_2), and the flow potential (S). According to the research results of electrical structure, there are high conductors and high resistance bodies in the crust of the Qinghai-Xizang Plateau and its surrounding areas, and violent earthquakes often occur at the junction of high conductors and high resistance bodies. Therefore, we choose σ_1 and σ_2 as 0.1 S/m and 0.01 S/m here. The flow potential generated by earthquake action is 0.1 to 10 V [35] [37], and 1 V is selected in this paper. Based on the above parameters and the coseismic sliding distribution shown in **Figure 2** (l is 54 km; a is 0 km; b is 25.3 km), the possible coseismic electromagnetic effects of the Dingri earthquake were calculated, as shown in **Figure 4**. Unlike the piezomagnetic effect, the range of magnetic field changes in the electrokinetic effect generated by the Dingri earthquake is relatively large. Magnetic fields greater than 0.1 nT are distributed along the rupture surface for about 300 km and perpendicular to the rupture surface for about 200 km. The electrokinetic effect magnetic field at the epicenter is +0.5 nT, and the magnetic fields at the two measuring points are +0.15 nT and −0.1 nT, respectively. The magnetic field changes at both ends of the rupture surface exceed 4 nT.

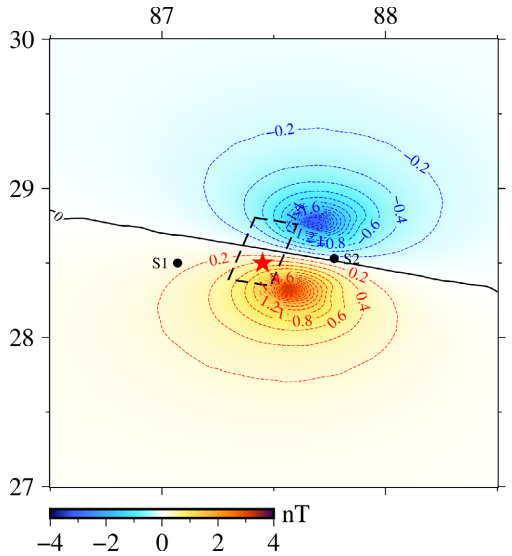

Figure 4. Coseismic electrokinetic fields expected from Dingri M6.8 earthquake.

The electrokinetic effect is not related to the sliding amount, but is closely related to the size of the sliding surface. The sliding distribution length used in this section is nearly 52 km, while some other models provide larger sliding surface sizes. The geothermal resources in southern Xizang are abundant, and there are hot water explosions, boiling springs, and other resources around the Dingri earthquake [38] [39], which may cause an increase in electrical conductivity [40]. During the post-earthquake investigation, a large number of sand blasting and water emitting phenomena were found, indicating that the source of the electrokinetic effect is not limited to the sliding surface. From this, it can be inferred that the variation range of the electrokinetic effect magnetic field is larger, which is sufficient to generate the magnetic field changes observed by the instrument. In particular, the S2 measuring point is located in the high gradient zone of the magnetic field.

4. Discussions

4.1. Lithosphere Magnetic Field Anomalies

Some researchers have analyzed the relationship between the lithospheric magnetic field and earthquakes and structures based on geomagnetic anomaly grid data (EMAG). Earthquakes usually occur in areas where the lithospheric magnetic field is weakly negative or at the junction of positive and negative anomalies [11] [13] [41], and important active faults are also located in the transition zone between positive and negative anomalies of the lithospheric magnetic field [12] [42]. Based on EMAG, the difference in lithospheric magnetic field between the two measurement points is about +18 nT, indicating that the lithospheric magnetic field at the two measurement points is basically the same. However, there is a significant difference from the measured results (about −120 nT). This difference may be due to that EMAG model incorporates no ground-based data and limited aeromagnetic data in the Tibetan Plateau region, relying primarily on satellite magnetic measurements that only reflect long-wavelength (>400 km) components of the lithospheric magnetic field. Furthermore, as satellite magnetic surveys are conducted at altitudes exceeding 300 km above the Earth's surface, the lithospheric magnetic field derived from the EMAG model in the Tibetan Plateau area is essentially an inverted result, which leads to significant deviations from actual ground observations. This article only used data from two measurement points, so it is unclear whether the two measurement points are located in the negative anomaly zone and the positive anomaly zone, respectively. Based on the EMAG, it is speculated that the range of differences in the lithospheric magnetic field in this area is relatively small and should belong to local magnetic anomalies.

The lithospheric magnetic field contains rich information on tectonic evolution, crustal structure, and seismogenic background [43]. The composition of the lithospheric material in the Dingri area is relatively complex, including the High Himalayan crystalline complex, the North Ao Formation greenschist to amphibolite metamorphic complex, and the southern Tibetan Tethys sedimentary rocks.

The boundaries of different lithologies are a series of normal faults [44] [45]. The S1 measurement point is located in the Tethys sedimentary rock area, while the epicenter and S2 measurement points are located in the high-grade metamorphic rock area of the High Himalaya, exposing ferromagnesian granulite [45]. Therefore, the magnetic susceptibility of the medium on the west side of the epicenter should be lower than that on the east side. Based on this, a simple crustal magnetic susceptibility model was established to calculate the possible lithospheric magnetic field (**Figure 5**). The side with high magnetic susceptibility has a larger magnetic field, while the side with low magnetic susceptibility has a smaller magnetic field, which is consistent with the measured results and confirms the difference in rock properties on both sides of the epicenter.

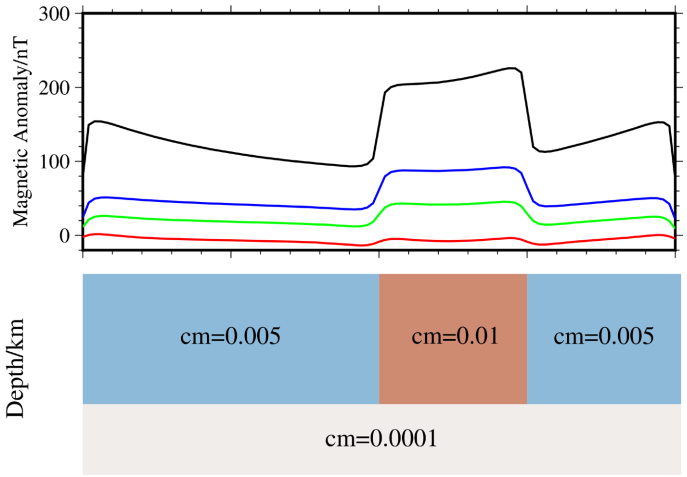

Figure 5. Forward simulation of the magnetic field resulted from magnetic substances. cm is the susceptibility of the medium. Red, green, blue, and black lines are the magnetic anomaly 2 km, 1 km, 0.5 km, and 0 km above ground, respectively.

The Dengmocuo fault, which gave birth to the Dingri 6.8 magnitude earthquake, is a relatively small normal fault in the southern Tibetan Rift system. It is located on the southern edge of the Xainza-Dingye fault zone and is one of the more active faults in the region [6] [46]. Many studies have shown that the normal faults within the southern Tibetan Rift system are regulated by the weak middle crust and serve as important channels for the exposure of lower crustal materials to the surface [2] [44]. The high Himalayan metamorphic rocks that appear locally in the Dengmocuo fault indicate that the fault displaced Tethys sedimentary rocks and became a channel for high Himalayan metamorphic rocks to fold back into the upper crust [45]. The low-velocity layer of the middle crust is widely distributed below the Dengmocuo fault, which may correspond to high-temperature partial melting or water-bearing fluids. The low-velocity body on the west side of the fault is more widely distributed [47], resulting in negative magnetic anomalies on the west side of the fault, causing the magnetic field of the lithosphere on the west side to be smaller than that on the east side.

4.2. Seismic Geomagnetic Anomalies

Research based on repeated observation data of the geomagnetic field shows that earthquakes often occur in areas with weak annual variations in the lithospheric magnetic field [22] [41] or in areas where the annual variations of the lithospheric magnetic field have been continuously changing for many years [48] [49]. This article is based on the repeated observation data of the geomagnetic field from 2018 to 2020. It was found that there was a significant turning point in the lithospheric magnetic field before the 6.8 magnitude earthquake, with an amplitude of about 6 nT. Is this an anomaly before the earthquake? A 5.9 magnitude earthquake occurred on March 20, 2020, with the epicenter located about 15 km northwest of the Dingri earthquake. Is the abnormal change in the lithospheric magnetic field discovered in this study related to the 2020 Dingri 5.9 magnitude earthquake?

From the quantitative calculation of the coseismic piezomagnetic effect and electrokinetic effect in the previous text, it can be seen that the piezomagnetic effect is mainly related to stress changes and the magnetic properties of the medium. Even with larger magnetic parameters, medium strong earthquakes such as the Dingri earthquake are difficult to generate geomagnetic field changes exceeding 1 nT at a distance of 20 km from the force source [50]. Therefore, pre-earthquake structural loading or micro-rupture stress disturbances are more difficult to produce significant geomagnetic field changes [48], which is different from some studies that suggest that pre-earthquake geomagnetic field anomalies may be related to stress changes [49].

The electrokinetic effect is mainly related to the distribution range of fluids, and fluid anomalies related to earthquakes usually have a wide distribution range. Fluid anomalies may exist within a range of several times the length of the fault rupture from the epicenter before and during the same earthquake [51], such as sustained water level anomalies and abnormal geomagnetic fields around the epicenter [52] [53]. Based on previous analysis, the electrokinetic effect may generate geomagnetic anomalies exceeding 1 nT, and the range is large. Therefore, the geomagnetic field anomaly before the earthquake may be related to the electrokinetic effect generated by underground fluid anomalies. The Dingri earthquake is more than 5 years away from the anomaly of the lithospheric magnetic field from 2018 to 2020. Statistical results on fluid and magnetic anomalies indicate that the pre-earthquake anomaly for a 6.8 magnitude earthquake can occur from several hours to several months, even 1 year [9] [51] [54], and the possibility of anomalies occurring 5 years or even longer before the earthquake is unlikely. Therefore, it is inferred that the anomaly of the lithospheric magnetic field from 2018 to 2020 should not be related to the Dingri earthquake, but is more likely to be related to the 5.9 magnitude Dingri earthquake in 2020. The distance between two geomagnetic measurement points for the 5.9 magnitude earthquake in Dingri is about 35 km, while statistical analysis results indicate that the possible pre-earthquake anomaly range for the 5.9 magnitude earthquake in Dingri is about 200 km [55].

Based on the quantitative calculations in the previous text, it can be seen that

significant magnetic field anomalies occur near faults and decay rapidly with distance. Although fluid and geomagnetic field anomalies before earthquakes may also occur in locations farther away from faults, the vast majority of anomalies occur in locations closer to faults. Therefore, setting up geomagnetic monitoring points near important faults makes it easier to observe magnetic field anomalies. At present, the geomagnetic repeated observation network is basically spatially uniformly distributed [56], which is advantageous for conducting research on the spatial distribution of the geomagnetic field and can observe some far-field anomalies, but it is not easy to observe more obvious near-fault anomalies.

Besides, temperature variations associated with seismic activity can also alter the geomagnetic field through thermomagnetic effects, where rock magnetism decreases with rising temperature and increases with cooling. According to Okubo *et al.* (2006) [57], temperature changes of several tens of degrees are required to generate significant magnetic variations (>1 nT), yet the magnitude of stress-induced thermal response is merely 1 mK/MPa [58], rendering the magnetic field changes caused by stress-derived temperature variations negligible. Whether other heat sources (e.g., heat transfer from subsurface fluid migration) could contribute to geomagnetic alterations remains unclear; future studies should incorporate regional thermal infrared anomalies, ground temperature data, and hydrological records to enable quantitative analysis.

5. Conclusions

This article uses geomagnetic field observation data obtained from 2018 to 2020 on both sides of the epicenter of the Dingri earthquake to analyze local lithospheric magnetic field anomalies. Based on the piezomagnetic effect and electrokinetic effects, the possible magnetic field anomalies caused by the Dingri earthquake were quantitatively calculated. The main conclusions are as follows:

(1) There is a difference of about −120 nT in the magnetic field of the lithosphere on the west and east sides of the epicenter of the Dingri earthquake, reflecting the different properties of the magnetic media on the east and west sides. The annual variation of the lithospheric magnetic field showed a significant turning point from −2.2 nT to +4 nT from 2018 to 2020, which may be a precursor anomaly before the earthquake. This anomaly should be related to the 5.9 magnitude earthquake in 2020.

(2) The magnitude and distribution range of the coseismic piezomagnetic field are relatively small, and even if the medium has strong magnetism, the magnetic field anomaly generated at the measuring point is only 0.3 nT. The magnitude and range of the electrokinetic effect are relatively large, with a maximum magnetic field of 4 nT at both ends of the fault and 0.5 nT at the epicenter. Considering the uncertainty of the sliding distribution, this effect may produce significant magnetic anomalies at the measuring point.

Acknowledgements

We thank the anonymous reviewers for their valuable comments and suggestions.

The study was supported by Hebei Earthquake Science and Technology Spark Program Project (Grant No. DZ2024112200008).

Conflicts of Interest

The authors declare no conflicts of interest regarding the publication of this paper.

References

[1] Shi, F., *et al.* (2025) Seismogenic Fault and Coseismic Surface Deformation of the Dingri MS6.8 Earthquake in Tibet, China. *Seismology and Geology*, **47**, 1-15.

[2] Pang, Y., Zhang, H., Shi, Y. and Gerya, T. (2022) Plume-Induced Rifting of Thickened Crust: 2D Numerical Model and Implications for N-S Rifts in Southern Tibet. *Geophysical Research Letters*, **49**, e2022GL101479. https://doi.org/10.1029/2022gl101479

[3] Shao, Z., Wu, Y., Ji, L., Diao, F., Shi, F., Li, Y., *et al.* (2023) Assessment of Strong Earthquake Risk in the Chinese Mainland from 2021 to 2030. *Earthquake Research Advances*, **3**, Article ID: 100177. https://doi.org/10.1016/j.eqrea.2022.100177

[4] Li, Q., *et al.* (2024) Estimated Seismic Source Parameters for 2020 Dingri MW5.6 Earthquake in Tibet and Study on the Stress Triggering. *Chinese Journal of Geophysics*, **67**, 172-188.

[5] Jin, Z. and Fialko, Y. (2021) Coseismic and Early Postseismic Deformation Due to the 2021 M7.4 Maduo (China) Earthquake. *Geophysical Research Letters*, **48**, e2021GL095213. https://doi.org/10.1029/2021gl095213

[6] Liu, D.S. and Li, M. (2024) Characteristics of Active Faults and Their Engineering Influence Analysis in Domestic Section of Shigatse-Jilong Railway. *Science Technology and Engineering*, **24**, 7327-7333.

[7] De Santis, A., Cianchini, G., Perrone, L., Soldani, M., Rahimi, H. and Alimoradi, H. (2025) Foundations for an Operational Earthquake Prediction System. *Geosciences*, **15**, Article No. 69. https://doi.org/10.3390/geosciences15020069

[8] Alimoradi, H., Rahimi, H. and De Santis, A. (2024) Successful Tests on Detecting Pre-Earthquake Magnetic Field Signals from Space. *Remote Sensing*, **16**, Article No. 2985. https://doi.org/10.3390/rs16162985

[9] Alimoradi, H., Rahimi, H. and Ovaisi Moaakhar, M. (2025) Investigation of Changes in the Cumulative Number of Magnetic Anomalies before and after Earthquakes Using Satellite Data. *Advances in Space Research*, **75**, 895-907. https://doi.org/10.1016/j.asr.2024.09.012

[10] Pulinets, S. and Herrera, V.M.V. (2024) Earthquake Precursors: The Physics, Identification, and Application. *Geosciences*, **14**, Article No. 209. https://doi.org/10.3390/geosciences14080209

[11] Feng, L.L., *et al.* (2017) Lithospheric Magnetic Field Feature of Sichuan-Yunnan Region and Its Relationship with Strong Earthquakes. *Journal of Seismological Research*, **40**, 352-356.

[12] Wen, L.M., *et al.* (2017) Crustal Magnetic Anomalies and Geological Structure in Yunnan Region. *Chinese Journal of Geophysics*, **60**, 3493-3504.

[13] Yang, X.H., Wang, B.H. and Yao, X.Y. (2020) Characteristics of Lithospheric Magnetic Field and Seismomagnetic Characteristics in Yunnan Area. *Journal of Seismological Research*, **43**, 745-750.

[14] Zhang, P., Du, J.S. and Li, H.P. (2024) CUG_CLMFM3Dv1: A High-Resolution Revised Spherical Cap Harmonic Model of Three-Dimensional Lithospheric Magnetic

Field over China and Surroundings. *Chinese Journal of Geophysics*, **67**, 1866-1880.

[15] Utada, H., Shimizu, H., Ogawa, T., Maeda, T., Furumura, T., Yamamoto, T., *et al.* (2011) Geomagnetic Field Changes in Response to the 2011 off the Pacific Coast of Tohoku Earthquake and Tsunami. *Earth and Planetary Science Letters*, **311**, 11-27. https://doi.org/10.1016/j.epsl.2011.09.036

[16] Song, C.K. and Zhang, H.Y. (2020) Analysis of Coseismic Variations in Magnetic Field of the Lushan MS7.0 Earthquake in 2013. *Seismology and Geology*, **42**, 1301-1315.

[17] Song, C., Zhang, P., Wang, C. and Chu, F. (2022) Piezomagnetic Anomalies Associated with the 2021 MW 7.3 Maduo (China) Earthquake. *Applied Sciences*, **12**, Article No. 1017. https://doi.org/10.3390/app12031017

[18] Okubo, K., Takeuchi, N., Utsugi, M., Yumoto, K. and Sasai, Y. (2011) Direct Magnetic Signals from Earthquake Rupturing: Iwate-Miyagi Earthquake of M7.2, Japan. *Earth and Planetary Science Letters*, **305**, 65-72. https://doi.org/10.1016/j.epsl.2011.02.042

[19] Yamazaki, K. (2013) Improved Models of the Piezomagnetic Field for the 2011 Mw9.0 Tohoku-Oki Earthquake. *Earth and Planetary Science Letters*, **363**, 9-15. https://doi.org/10.1016/j.epsl.2012.12.019

[20] Ni, Z., *et al.* (2014) Research on Anomalies Variation of Lithosphere Magnetic Field before and after Lushan MS7.0 Earthquake. *Journal of Seismological Research*, **37**, 61-65.

[21] Cai, S.S. and Chen, B. (2022) Statistical Analysis of the Annual Variation of the Lithospheric Seismomagnetic Anomaly in Chinese Mainland. *Journal of Seismological Research*, **45**, 592-598.

[22] Zhang, H.Y. (2024) Abnormal Variation of Lithospheric Magnetic Field before the Ping-Yuan MS5.5 Earthquake in Shandong Province and Its Seismogenic Mechanism. *Journal of Geodesy and Geodynamics*, **44**, 892-898.

[23] Johnston, M.J.S., Sasai, Y., Egbert, G.D. and Mueller, R.J. (2006) Seismomagnetic Effects from the Long-Awaited 28 September 2004 M6.0 Parkfield Earthquake. *Bulletin of the Seismological Society of America*, **96**, S206-S220. https://doi.org/10.1785/0120050810

[24] Chen, Z.Y., *et al.* (2024) Analysis Based on the Meta-Instability Theory of the Variation Characteristics of the Lithospheric Magnetic Field in Yunnan before the 2021 Yangbi, Yunnan MS6.4 Earthquake. *Journal of Seismological Research*, **44**, 391-398.

[25] Hattori, K., Takahashi, I., Yoshino, C., Isezaki, N., Iwasaki, H., Harada, M., *et al.* (2004) ULF Geomagnetic Field Measurements in Japan and Some Recent Results Associated with Iwateken Nairiku Hokubu Earthquake in 1998. *Physics and Chemistry of the Earth, Parts A/B/C*, **29**, 481-494. https://doi.org/10.1016/j.pce.2003.09.019

[26] Wang, Z., Yuan, J., Chen, B., Chen, S., Wang, C. and Mao, F. (2019) Local Magnetic Field Changes during Gas Injection and Extraction in an Underground Gas Storage. *Geophysical Journal International*, **217**, 271-279. https://doi.org/10.1093/gji/ggz012

[27] Gu, Z.W., *et al.* (2009) Research of Geomagnetic Spatial-Temporal Variations in China by the NOC Method. *Chinese Journal of Geophysics*, **52**, 2602-2612.

[28] Chen, B., *et al.* (2017) Data Processing Flowchart of Chinese Mobile Geomagnet Monitoring Array. *Journal of Seismological Research*, **40**, 335-339.

[29] Su, S.P., Chen, S.G. and Zhao, H.Q. (2022) Taylor Polynomial Spatial Reference Field Method for Field Geomagnetic Diurnal Variation Reduction. *Izvestiya, Physics of the Solid Earth*, **58**, 981-991. https://doi.org/10.1134/s1069351322110015

[30] Wang, M. and Shen, Z. (2020) Present-Day Crustal Deformation of Continental

China Derived from GPS and Its Tectonic Implications. *Journal of Geophysical Research*: *Solid Earth*, **125**, e2019JB018774. https://doi.org/10.1029/2019jb018774

[31] Song, C.K. and Chen, B. (2024) Heterogeneity Effect of Elastic Properties on Piezomagnetic Fields Associated with Dislocation Source. *Izvestiya*, *Physics of the Solid Earth*, **60**, 325-332. https://doi.org/10.1134/s1069351324700381

[32] Yamazaki, K. (2021) Piezomagnetic Fields Associated with a Dislocation Source in a Layered Elastic Medium. *Geophysical Journal International*, **226**, 2032-2056. https://doi.org/10.1093/gji/ggab160

[33] International Geomagnetic Reference Field (IGRF). https://www.ncei.noaa.gov/products/international-geomagnetic-reference-field

[34] Preliminary Result for Rupture Process of Jan. 7, 2025, M6.8 Earthquake, Rikaze, China. https://itpcas.cas.cn/new_kycg/new_kyjz/202501/t20250107_7514999.html

[35] Fitterman, D.V. (1979) Theory of Electrokinetic-Magnetic Anomalies in a Faulted Half-Space. *Journal of Geophysical Research*: *Solid Earth*, **84**, 6031-6040. https://doi.org/10.1029/jb084ib11p06031

[36] Murakami, H. (1989) Geomagnetic Fields Produced by Electrokinetic Sources. *Journal of Geomagnetism and Geoelectricity*, **41**, 221-247. https://doi.org/10.5636/jgg.41.221

[37] Hanks, T.C. (1974) Constraints on the Dilatancy-Diffusion Model of the Earthquake Mechanism. *Journal of Geophysical Research*, **79**, 3023-3025. https://doi.org/10.1029/jb079i020p03023

[38] Li, Z.Q., *et al.* (2005) Characteristic and Distribution of the Partial Melting Layers in the Upper Crust: Evidence from Active Hydrothermal Fluid in the South Tibet. *Acta Geologica Sinica*, **79**, 68-77.

[39] Wang, C.G., *et al.* (2024) Hydrochemical Characteristics and Origin of Geothermal Fluids in the Guduihigh-Temperature Geothermal System in Comei County, Southern Tibet. *Acta Geologica Sinica*, **98**, 558-578.

[40] Ye, G.F., Jin, S. and Wei, W.B. (2007) Wait Research of Conductive Structure of Crust and Upper Mantle beneath the South-Central Tibetan Plateau. *Earth Science-Journal of China University of Geosciences*, **32**, 491-498.

[41] Gu, C.L., *et al.* (2010) Analysis of the Variation Characteristic in the Lithospheric Geo-Magnetic Field before and after Earthquakes. *Progress in Geophysics*, **25**, 472-477.

[42] Chen, Z.Y., *et al.* (2024) Study on the Relationship between Lithospheric Magnetic Field and Geological Structure and Seismic Activity: Taking the 2021 Ms6.4 Yangbi Earth-Quake as an Example. *Seismology and Geology*, **46**, 449-461.

[43] Zhao, J.M. (2004) Structure of Lithospheric Density and Geomagnetism beneath the Tianshan Orogenic Belt and Their Geodynamic Implications. *Chinese Journal of Geophysics*, **47**, 1061-1067.

[44] Liu, Y., *et al.* (2004) Characteristics of the Main Central Thrust and Southern Tibetan Detachment in the Tingri Area, Southern Tibet, and Ages of Their Activities. *Geological Bulletin of China*, **23**, 636-644.

[45] Chu, Y., Guo, Y., Liu, T., Liu, X., Hu, F., Lei, Y., *et al.* (2024) South Tibetan Detachment System Activity and Leucogranite Emplacement: Insights from the Shisha Pangma Regions. *Acta Petrologica Sinica*, **40**, 1461-1474. https://doi.org/10.18654/1000-0569/2024.05.08

[46] Caibayangzeng and Zhao, J.M. (2018) A Summary of Researches on Southern Tibet Rift System. *Journal of Seismological Research*, **41**, 14-21.

[47] Huang, S., Yao, H., Lu, Z., Tian, X., Zheng, Y., Wang, R., *et al.* (2020) High-Resolution 3-D Shear Wave Velocity Model of the Tibetan Plateau: Implications for Crustal Deformation and Porphyry Cu Deposit Formation. *Journal of Geophysical Research*: *Solid Earth*, **125**, 1-17. https://doi.org/10.1029/2019jb019215

[48] Song, C.K., Zhang, P.T. and Chen, B. (2024) Geomagnetic Field Change before and after Maduo MW7.3 Earthquake Based on Repeat Geomagnetic Measurement Data. *Journal of Institute of Disaster Prevention*, **26**, 38-46.

[49] Wang, Z.J., Li, B. and Su, S.P. (2024) Analysis of the Seismomagnetic Anomaly of the Tangshan MS5.1 Earthquake Based on the Accumulative Variation of the Lithospheric Magnetic Field. *Journal of Seismological Research*, **47**, 517-527.

[50] Mueller, R.J. and Johnston, M.J.S. (1998) Review of Magnetic Field Monitoring near Active Faults and Volcanic Calderas in California: 1974-1995. *Physics of the Earth and Planetary Interiors*, **105**, 131-144. https://doi.org/10.1016/s0031-9201(97)00086-1

[51] Yan, R., *et al.* (2018) Review and Statistically Characteristic Analysis of Underground Fluid Anomalies Prior to the 2008 Wenchuan MS8.0 Earthquake. *Chinese Journal of Geophysics*, **61**, 1907-1921.

[52] Li, Q., Lin, Y.F. and Zeng, X.P. (2006) Wavelet Analysis as a Tool for Revealing Geomagnetic Precursors of the Zhangbei Earthquake. *Chinese Journal of Geophysics*, **49**, 855-863.

[53] Zhang, L., *et al.* (2016) Characteristics of Geomagnetic Regular Diurnal Variation before Wenchuan Earthquake. *Chinese Journal of Geophysics*, **59**, 952-958.

[54] De Santis, A., Marchetti, D., Pavón-Carrasco, F.J., Cianchini, G., Perrone, L., Abbattista, C., *et al.* (2019) Precursory Worldwide Signatures of Earthquake Occurrences on Swarm Satellite Data. *Scientific Reports*, **9**, Article No. 20287. https://doi.org/10.1038/s41598-019-56599-1

[55] Dobrovolsky, I.P., Zubkov, S.I. and Miachkin, V.I. (1979) Estimation of the Size of Earthquake Preparation Zones. *Pure and Applied Geophysics*, **117**, 1025-1044. https://doi.org/10.1007/bf00876083

[56] Chen, B., Yuan, J., Ni, Z. and Wang, C. (2022) Chinese Geomagnetic Reference Field 2020 by the Revised Surface Spline Method. *Applied Sciences*, **12**, Article No. 2297. https://doi.org/10.3390/app12052297

[57] Okubo, A., Kanda, W. and Ishihara, K. (2006) Numerical Simulation of Volcano Magnetic Effects Due to Hydrothermal Activity. *Disaster Prevention Research Institute Annuals*, **49**, 211-217.

[58] Yang, X., Lin, W., Tadai, O., Zeng, X., Yu, C., Yeh, E., *et al.* (2017) Experimental and Numerical Investigation of the Temperature Response to Stress Changes of Rocks. *Journal of Geophysical Research*: *Solid Earth*, **122**, 5101-5117. https://doi.org/10.1002/2016jb013645